/
Article / Book Information

Title	CONTROL-FORCE PREDICTION SPECTRUM FOR BASE-ISOLATED BUILDINGS WITH FEEDBACK CONTROL
Authors	Y. Chen, D. Sato, K. Miyamoto, J. She
Pub. date	2020, 9
Citation	2020 17WCEE Proceedings

CONTROL-FORCE PREDICTION SPECTRUM FOR BASE-ISOLATED BUILDINGS WITH FEEDBACK CONTROL

Y. Chen[1], D. Sato[2], K. Miyamoto[3] and J. She[4]

[1] *Graduate student, Tokyo Institute of Technology, chen.y.at@m.titech.ac.jp*
[2] *Associate Professor, Tokyo Institute of Technology, sato.d.aa@m.titech.ac.jp*
[3] *Researcher, Shimizu Corporation, kou_miyamoto@shimz.co.jp*
[4] *Professor, Tokyo University of Technology, sato.d.aa@m.titech.ac.jp*

Abstract

Passive-base-isolation (PBI) structures are widely used to minimize damage to superstructures and resume operation immediately after violent earthquakes. In recent years, the combination of PBI and active structural control (ASC) has been employed in many buildings globally to improve control performance. While estimating of the required control force is important to select an appropriate actuator to perform ASC, previous approaches utilized trial-and-error because the dependency of the maximum control force on the natural period of the control system and the passive damper has not been expressed theoretically. Sato et al. proposed a control-force spectrum for PBI buildings combined with linear-quadratic-regulator (LQR) control. Their method estimates the maximum control force without any numerical simulations, simplifying the design procedure for the controller. However, the method used by Sato et al. is only suited for LQR control and it cannot adjust the natural period of the control system, limiting its applicability. This study promotes the concept of control-force spectrum proposed by Sato et al. to feedback control and adjusts both the natural period and damping ratio for the control system (control-force prediction spectrum). To devise the control-force spectrum, the equivalent model of the ASC system is constructed to theoretically describe the dependency of the vibration characteristics of the control system on the feedback gain. Using the equivalent model and control-force spectrum, both the maximum response and maximum control are estimated without additional numerical simulations. Therefore, it simplifies selection of the natural period, passive damper, and maximum control force. We also develop a control-system design method for a single-degree-of-freedom (SDOF) model using the control-force spectrum. This design method calculates the range of the combination of the natural period, passive damper, and maximum control force that satisfies the restrictions. This method requires neither trial-and-error nor numerical simulations, thus, simplifying the design procedure. Since the PBI layer of a PBI building is much softer than the superstructure, PBI buildings can usually be considered as SDOF models. Therefore, this method can be used to design PBI buildings with ASC. Numerical examples validate the efficacy of the control-force prediction spectrum.

Keywords: base-isolated buildings; active structural control; maximum control force; equivalent model; design method

1. Introduction

Passive-base-isolation (PBI) structures are used to minimize damage to superstructures and resume operation immediately after violent earthquakes. Their use increased sharply in Japan after the Great Hanshin earthquake of 1995 [1]. The PBI structure approach is popular throughout the world for applications like public buildings and other important facilities [2,3]. In recent years, safety demands for many structures, and especially nuclear power plants, have grown, so the application of PBI structure to nuclear power plants is a topic of worldwide research [4,5]. Unfortunately, it is difficult to suppress the displacement response within the allowance range for a PBI structure because the natural period of the PBI layer is relatively long [6,7]. To solve this problem, we need to increase the damping of the PBI layer, for example, adding passive viscous dampers to the PBI layer. However, the restriction of the space of the PBI layer causes difficulty in achieving a high damping ratio. To simultaneously satisfy the criteria of displacement and absolute acceleration during a violent earthquake, it is attractive to consider the addition of active structural control (ASC) to the PBI layer to increase the damping.

When ASC is applied in structural control, the required control force is quite large, making the estimation of the maximum control force very important in selecting the actuator. Moreover, the control system also mainly designed by the trial-and-error approach, which creates great pressure to come up with numerical simulations. We therefore need an analytical method to estimate the maximum control force. The response spectra, expressing the dependency of the maximum response to the natural period and damping ratio for a passive model, are widely used in structural design to select the desired vibration characteristic. If the concept of response spectra can be broadened to the estimation of the maximum control force for a PBI model with ASC, the selection of the natural period, passive damper, and actuator will be simplified. To realize this idea, we consider the equivalent model to express the vibration characteristics of an active model (a model with ASC).

Sato et al. proposed a control-force spectrum that theoretically estimates the maximum control force of single degree-of-freedom (SDOF) active structural control systems [8] only using the velocity response spectrum of the earthquake. However, the research performed by Sato et al. only adjusts the damping ratio of the model and only suits for LQR control, limiting its applicability. Horiguchi et al. developed a method that simultaneous optimize the structures and control systems for SDOF models with LQR control [9]. The method proposed by Horiguchi et al. estimates the maximum control force considering the adjustment of natural period and damping ratio of control system. However, the research performed by Horiguchi et al. did not show the estimation error of their method and did not broaden this method to the spectrum, making it difficult using at the design stage.

This paper devises a control-force prediction spectrum, theoretically expressing the dependency of the maximum control force to the natural period and damping ratio, using only the displacement response spectrum, velocity response spectrum, and no additional numerical simulations. The control-force prediction spectrum simplifies selection of the natural period, damping ratio, and maximum control force. To devise the control-force spectrum, the equivalent model of the active model is constructed. We also propose a control-system design method for an SDOF model using the control-force spectrum. The design method calculates the range of the combination of the natural period, passive damper, and maximum control force that satisfies the restrictions. This method requires neither trial-and-error nor numerical simulations. So, it simplifies the design procedure. Since the PBI layer of a PBI building is much softer than the superstructure, PBI buildings can usually be considered as SDOF models [10]. Therefore, this method can be used to design a PBI building with ASC.

2. Control system and Equivalent model

2.1 Control system

The model used in this study is an SDOF model. The dynamics of an SDOF control system are described by the following equation:

2

$$m\ddot{x}(t) + c\dot{x}(t) + kx(t) = d(t) - u(t) \,, \tag{1}$$

where m, k, and c are the mass, stiffness-coefficient, and damping-coefficient of the structure respectively; x is the displacement response; d and u are disturbance force and control force, respectively. k and c are defined by

$$k = \frac{4\pi^2 \cdot m}{T^2}, \text{ and } c = 2\zeta\sqrt{mk} \,, \tag{2a, b}$$

where T and ζ are the natural period and damping ratio of the structure, respectively. The state-space representation of (1) is

$$\dot{z}(t) = Az(t) + B_d d(t) - B_u u(t) \tag{3}$$

where z is the state vector; A is a system matrix; B_u is the input matrix for u; B_d is the input matrix for d. z, A, B_u, and B_d are defined by

$$z(t) = \begin{bmatrix} x(t) \\ \dot{x}(t) \end{bmatrix}, \quad A = \begin{bmatrix} 0 & 1 \\ -k/m & -c/m \end{bmatrix}, \text{ and } B_d = B_u = \begin{bmatrix} 0 \\ 1/m \end{bmatrix}. \tag{4}$$

Feedback control law

$$u(t) = \begin{bmatrix} K_{P1} & K_{P2} \end{bmatrix} z(t) = K_{P1}x(t) + K_{P2}\dot{x}(t) \tag{5}$$

is used, where K_P is the state-feedback gain; K_{Pi} is the ith element of K_P.

Fig. 1 shows the block-diagram of the control system used in this study.

2.2 Equivalent model

In this paper, the equivalent model is defined as a model with a linear spring and dash-pot, and the responses of the equivalent model are the same as those of the active model (a model with ASC device) [Fig. 0, $x_{eq}(t) = x(t)$]. This section constructs the equivalent model of the control system theoretically clarifying the relationship between the feedback gain and vibration characteristics.

Substituting (5) into (1) gives the vibration equation of the equivalent model:

$$m\ddot{x}(t) + c_{eq}\dot{x}(t) + k_{eq}x(t) = d(t) - u(t) \,, \tag{6}$$

where k_{eq} and c_{eq} represent the stiffness coefficient and damping coefficient of the equivalent model:

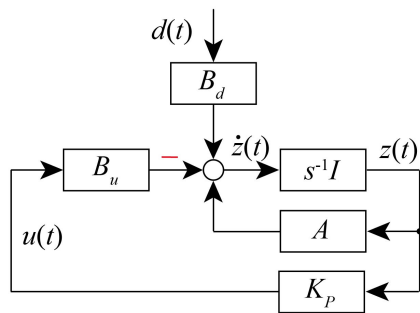$$k_{eq} = k + K_{P1} \,, \text{ and} \tag{7a}$$

Fig. 1 Block diagram

(a) Active model   (b) Equivalent model

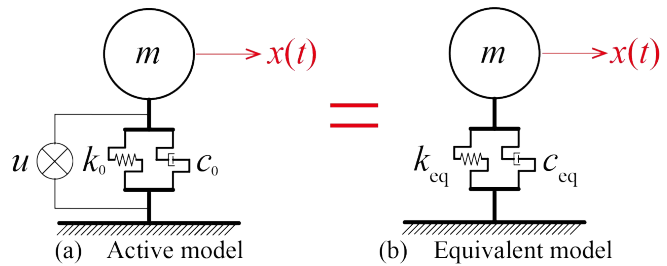Fig. 2 Active model and equivalent model

3

$$c_{eq} = c + K_{P2}. \tag{7b}$$

Using (7), we theoretically express the dependencies of the stiffness coefficient and the damping coefficient of the equivalent model on the entries of the feedback gain.

From (7a), it can be seen that k_{eq} is dependent on k and K_{P1}. When $K_{P1} = 0$, the value of k_{eq} is equal to k, and the value of k_{eq} increases as K_{P1} increases. From (7b), it can be seen that c_{eq} is dependent on c and K_{P2}. When $K_{P2} = 0$, the value of c_{eq} is equal to c, and the value of c_{eq} increases as K_{P2} increases. Moreover, as is commonly known, the natural angular frequency ω_{eq}, natural period T_{eq}, and damping ratio ζ_{eq} of the equivalent model are

$$\omega_{eq} = \sqrt{\frac{k_{eq}}{m}}, \tag{8a}$$

$$T_{eq} = \frac{2\pi}{\omega_{eq}}, \text{ and} \tag{8b}$$

$$\zeta_{eq} = \frac{c_{eq}}{2m\omega_{eq}}. \tag{8c}$$

In addition, solving (7) yields a calculation formula for the determination of the feedback gain to achieve desired vibration characteristics:

$$K_{P1} = k_{eq} - k, \text{ and} \tag{9a}$$

$$K_{P2} = c_{eq} - c. \tag{9b}$$

3. Control-force prediction spectrum

3.1 Derivation of the prediction control-force spectrum

Response spectra, which express the dependency of the maximum responses of an SDOF model to the natural period and damping ratio under an earthquake, are widely used in structural design. The maximum control force is, however, mainly estimated by trial-and-error approaches, generating a great demand of numerical simulations to determine the natural period, passive damper, and required control force. This section devises the control-force spectrum considering the combination of PBI and ASC, which expresses the dependency of the maximum control force on the natural period and passive damper. The derivation of the control-force spectrum uses only the velocity-response spectrum of an earthquake and requires no additional numerical simulations.

Since the response of the equivalent model is equal to that of the active model, the control force is estimated by the difference between (6) and (1):

$$u(t) = (k_{eq} - k)x(t) + (c_{eq} - c)\dot{x}(t), \tag{10}$$

and the maximum control force, u_{max}, is

$$u_{max} = \max\left\{(k_{eq} - k)x(t) + (c_{eq} - c)\dot{x}(t)\right\}. \tag{11}$$

Since the maximum value of displacement response and velocity response usually do not appear at the same time, the maximum control (11) yields

4

$$u_{\max} \le \max\left\{(k_{eq}-k)x(t)\right\} + \max\left\{(c_{eq}-c)\dot{x}(t)\right\}$$
$$= (k_{eq}-k)\max\left\{x(t)\right\} + (c_{eq}-c)\max\left\{\dot{x}(t)\right\} \qquad (12)$$

The maximum responses of the equivalent model can be estimated by the response spectra of the earthquake

$$\max\left\{x(t)\right\} = S_D\left(T_{eq},\,\zeta_{eq}\right),\text{ and }\max\left\{\dot{x}(t)\right\} = S_V\left(T_{eq},\,\zeta_{eq}\right). \qquad (13)$$

where $S_D(T_{eq},\,\zeta_{eq})$ and $S_D(T_{eq},\,\zeta_{eq})$ are the values of the displacement response spectrum and velocity response spectrum, respectively. Substituting (13) into (12) yields

$$u_{\max} \le (k_{eq}-k)S_D\left(T_{eq},\,\zeta_{eq}\right) + (c_{eq}-c)S_V\left(T_{eq},\,\zeta_{eq}\right). \qquad (14)$$

By dividing (12) by the weight of the model *mg*, the maximum shear-force coefficient of the control force $C_{u,\max}$ is obtained:

$$C_{u,\max} = \frac{u_{\max}}{mg} \le \frac{(k_{eq}-k)}{mg}S_D\left(T_{eq},\,\zeta_{eq}\right) + \frac{(c_{eq}-c)}{mg}S_V\left(T_{eq},\,\zeta_{eq}\right) = C_{u,D} + C_{u,V}. \qquad (15)$$

where

$$C_{u,D} = \frac{(k_{eq}-k)}{mg}S_D\left(T_{eq},\,\zeta_{eq}\right)\text{ and }C_{u,V} = \frac{(c_{eq}-c)}{mg}S_V\left(T_{eq},\,\zeta_{eq}\right). \qquad (16)$$

From (16), the maximum shear-force coefficient contains both the component of displacement response, S_D, and the velocity response, S_V. Since, maximum value of displacement response and velocity response usually do not appear at the same time, this study uses the square root of sum of squares (SRSS) to estimate maximum shear-force coefficient of the control force:

$$_pS_C\left(T,T_{eq},\zeta,\zeta_{eq}\right) := \sqrt{C_{u,D}^2 + C_{u,V}^2} \approx C_{u,\max}. \qquad (17)$$

Because (17) estimates the maximum shear-force coefficient of the control force, it is defined as the control-force spectrum $_pS_C$, and is a function of the natural period of the structure T, the damping ratio of the structure ζ, the equivalent natural period T_{eq}, and the equivalent damping ratio ζ_{eq}.

The control-force prediction spectrum, (17), theoretically expresses the dependency of the maximum control force to the natural period of structure, damping ratio of structure, equivalent natural period, and equivalent damping ratio by using displacement-response spectrum and velocity-response spectrum under a certain earthquake wave and needs no additional numerical simulations.

3.2 Numerical verification of the control-force spectrum

This section shows the control-force prediction spectrum $_pS_C$ of Taft NS (Fig. 3), El Centro 1940 NS (Fig. 4), and JMA Kobe NS (Fig. 5). The model used in this section is presented in Table 1.

Disturbance force $d(t)$ is calculated by the following equation:

$$d(t) = -m\ddot{x}_g(t). \qquad (18)$$

where is ground acceleration of earthquakes.

Fig. 6 presents the accuracy of the prediction control-force spectrum of Taft NS, El Centro 1940 NS, and JMA Kobe NS. In addition, the values of S_C in Fig. 6 use simulation results and the values of $_pS_C$ use (). From Fig. 6, it can be seen that the error of the control-force prediction is less than 20% of the 3 examples.

5

Fig. 7 presents the control-force spectrum of Taft NS, El Centro 1940 NS, and JMA Kobe NS. From Fig. 7, the following results are obtained:

(1) The maximum control force increases as the peak ground acceleration of earthquake increases to achieve the desired vibration characteristics.

(2) The maximum control force increases as the equivalent damping ratio increases, if $T = T_{eq}$.

(3) The maximum control force decreases as the equivalent damping ratio increases for the resonance range.

(4) The maximum control force decreases as the equivalent natural period increases expect for the resonance range.

4. Design method

This section develops a design method for the PBI structure combined with ASC for determining the natural period, passive damper, and maximum control force, that satisfies these restrictions using the calculation formulas for weighting matrices (9) and the prediction control-force spectrum (17). Moreover, the design of the PBI reactor combined with ASC demonstrates the validity of the design method. Using this

Table 1   Parameters of the model

Parameter	Symbol	Value
mass	m	1.00 kg
stiffness	k	2.46 N/m
damping coefficient	c	0.03 Ns/m

(a)   accelerogram

(b)   velocity response spectrum

Fig. 3   Taft NS wave

(a)   accelerogram

(b)   velocity response spectrum

Fig. 4   El Centro wave

(a)   accelerogram

(b)   velocity response spectrum
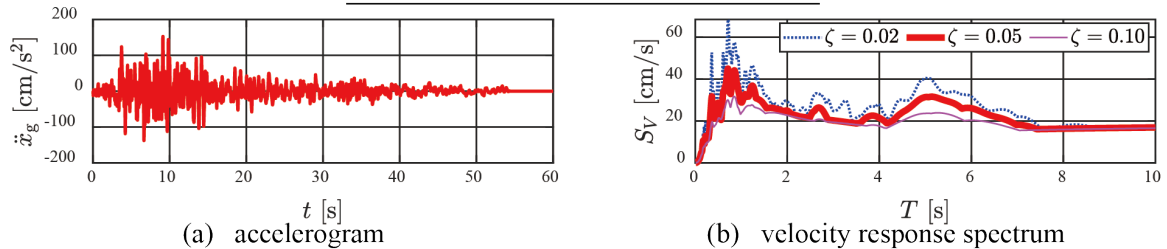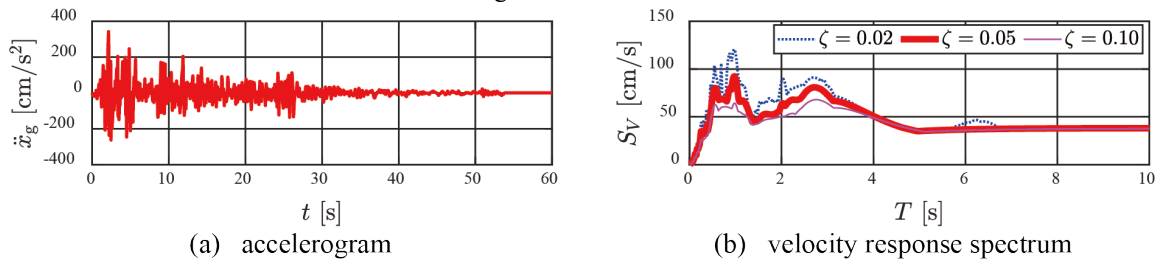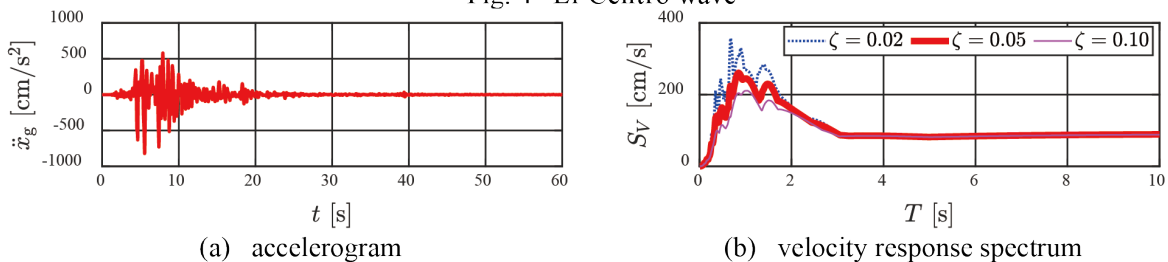
Fig. 5   JMA Kobe wave

6

design method, the natural period cannot be adjusted by ASC. However, if the structure is a PBI structure, the natural period of the control system can be adjusted by the PBI layer.

4.1 Design algorithm

Step 0.   Specify the design conditions:

Earthquake waves used in design procedure Mass of structure

Limitation of the maximum displacement response, maximum velocity response, and maximum absolute acceleration response

Limitation of natural period and damping ratio of structure

Limitation of shear-force coefficient of control force

Step 1.   From the response spectrum, select the equivalent model (equivalent natural period T_{eq} and equivalent damping ratio ζ_{eq}) that satisfies the limitation conditions of the responses (displacement, velocity, and absolute acceleration) in Step 0.

Step 2.   Verify whether the selected equivalent model satisfies the limitation conditions of the natural period of the structure T, damping ratio of the structure ζ, and the maximum shear-force coefficient for control force $C_{u,lim}$ and by using the control force spectrum (17). If the limitation conditions are met, specify natural period of the structure T, damping ratio of the structure ζ, and go to the next step. If not, go back to Step 1 and select another equivalent model.

Step 3.   Using (8) and equivalent natural period T_{eq} and equivalent damping ratio ζ_{eq} to calculate the equivalent stiffness k_{eq} and the equivalent damping coefficient c_{eq}.
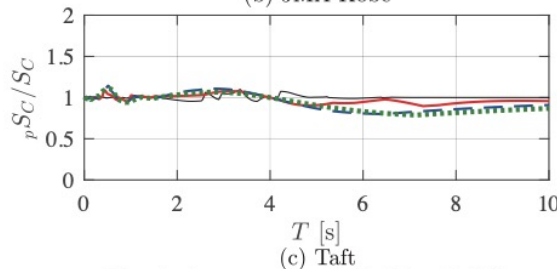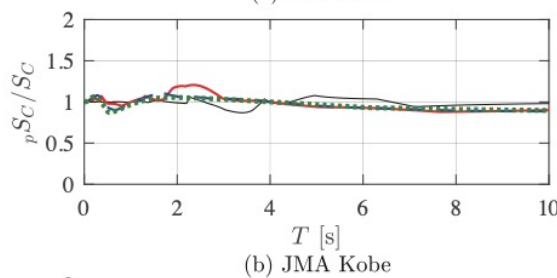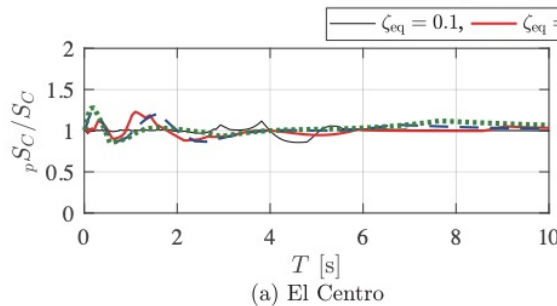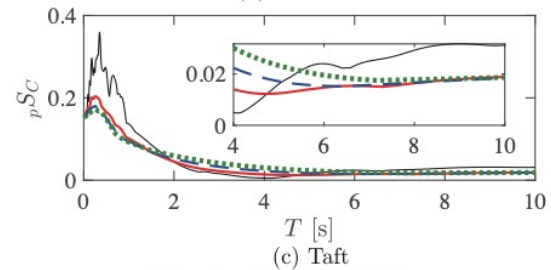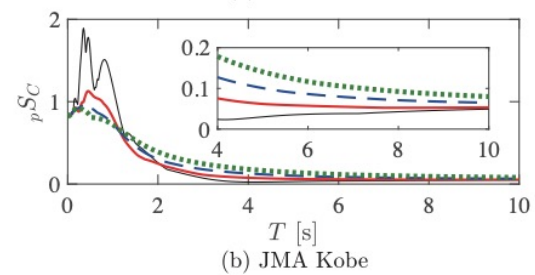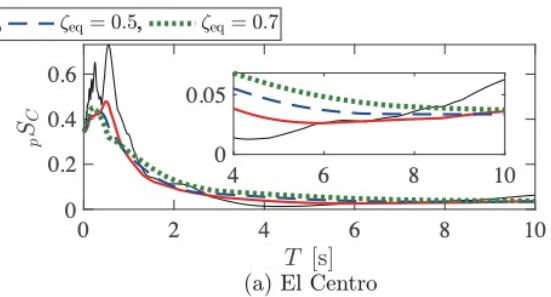

Fig. 6 Accuracy of $_pS_C$ ($\zeta = 0.01$)

Fig. 7 $_pS_C$ ($\zeta = 0.01$)

Step 4.   Using the equivalent stiffness k_{eq} and the equivalent damping coefficient c_{eq} determined in Step 3, calculate the state feedback gain K_P by (9).

5. Conclusion

This study first constructed an equivalent model of an active model (control system), and theoretically expressed the dependency of vibration characteristics to feedback gain. Then, using the equivalent model, we calculate the prediction control-force spectrum, which theoretically expresses the dependency of the maximum control force to the natural period of the structure, damping ratio of structure, equivalent natural period, and equivalent damping. The calculation of the prediction control-force spectrum only uses the response spectra of earthquakes and needs no additional numerical simulations. This paper also develops the design method, which shows how to determine the maximum control force and passive damper, which satisfies the restrictions thus eliminating the trial-and-error approach and numerical simulation. This study clarified following 3 points:

(1) The 1st entry of the feedback gain, K_{P1}, effects the equivalent stiffness of the equivalent model, k_{eq}, and the 2nd entry of the feedback gain, K_{P2}, effects the equivalent damping coefficient of the equivalent model, c_{eq}. The value of k_{eq} increases as the value of K_{P1} increases, and the value of c_{eq} increases as the value of K_{P2} increases.

(2) Because the vibration characteristics of the active model are the same as those of equivalent model, the maximum response is estimated by the equivalent model using response spectra.

(3) By using the prediction control-force spectrum the required maximum control force can be estimated at the design stage without trial-and-error or any numerical simulations, so it simplifies the design of the control system.

6. References

[1] Tanaka Y, Fukuwa N, Tobita J, Mori M: Development and analysis of database for base-isolated buildings in japan [in Japanese]. *AIJ J Technol Des 2011*, **17**(35), 79–84.

[2] Soto MG, Adeli H: Vibration control of smart base-isolated irregular buildings using neural dynamic optimization model and replicator dynamics. *Engineering Structures*, 2018, **156**, 322–36.

[3] Warn GP, Ryan KL: A review of seismic isolation for buildings: Historical development and research needs. *Buildings*, 2012, **2**(3), 300–25.

[4] Ryu S, Yoshito U, Yoshito U: A study on seismic behavior of isolated reactor building in large input region. Part 1: Overall outline [in Japanese]. I *Summaries of technical papers of annual meeting of Architectural Institute of Japan* (2013), 1285–1286.

[5] Takemi N, Shingo A, Hiroki H, Shinichiro N, Yoshito U, Ryu S: A study on seismic behavior of isolated reactor building in large input region. Part 3: Fail-safe system incorporated lead rubber bearing [in Japanese], *Summaries of technical papers of annual meeting of Architectural Institute of Japan* (2013), 1285–1286.

[6] Asano H, Hirotani T, Nakayama T, Norimono T, Aikawa Y, Sato K, et al.: Development of an evaluation method for seismic isolation systems of nuclear power facilities: Part 10 Evaluation of seismic isolator design. *Proceedings of ASME 2014 pressure vessels & piping conference* (2014), **8**, V008T08A017.

[7] Kumar M, Whittaker AS. Effect of seismic hazard definition on isolation-system displacements in nuclear power plants. *Engineering Structures*, 2017;148:424–35.

[8] Daiki S, Yinli C, Miyamoto K, Jinhua S: A spectrum for estimating the maximum control force for passive-base-isolated buildings with LQR control, *Engineering Structures*, **199**, 2019.

[9] Kohiyama…

8

[10] Architectural of Institute of Japan: Design Recommendations for Seismically Isolated Buildings (2016), *Architectural of Institute of Japan*, 5ᵗʰ edition.